

Early Warning System for Landslide Risk and SHM by Means of Reinforced Optic Fiber in Lifetime Strain Analysis

Renato Zona, Martina De Cristofaro, Luca Esposito, Paolo Ferla, Simone Palladino,
Elena Totaro, Lucio Olivares and Vincenzo Minutolo
Università della Campania "L. Vanvitelli", via Roma 29, Aversa(CE), Italy

Keywords: Early Warnings, Big Data, BODTA, Soil Movement, Sensors Network, Internet of Things, Strain, Displacement, Structure Health Monitoring.

Abstract: Nowadays Sensors Networks (SN) are intensively used for environment monitoring and structural health monitoring. Sensors Network can be greatly useful for data collection in hazard sites or sites of cultural heritage. For the latter is meant structure with historical value as masonry ancient construction, while the first one has to be intended as landslide risk zone. Collecting data in terms of strain and displacements is particularly crucial when anticipating the risks of disasters. When integrated into the Internet of Things and a Big Data database, the SN offers an innovative way to have a health state of the monitored site. The paper describes a prototype of a land-sliding risk early warning system hosted that consists of an optical fiber sensor, called S.T.R.A.I.N, that collects values of deformations in soils or structures in time continuous analysis. This offers an online database readable in remote control from a server or a smartphone. The developed prototype collects and displays strain values, soil movement and structure displacements.

1 INTRODUCTION

The basis of structural health monitoring (SHM) has been laid by Housner et al. (Housner, et al., 1997), where it is defined as the continuous measurement and analysis of the main structural and environmental parameters under operating conditions in order to detect anomalous behavior of structures in the initial phases and then as a prevention tool.

Sensors Network can be greatly useful for data collection in several hazard sites: the field of Cultural Heritage is probably one of the most emblematic of the potentialities offered today by modern techniques and methods of surveying and monitoring. In the past few years, applications of Sensor Networks (SNs), Wireless Sensor Networks (WSNs) and their modern variant offered by the Internet of Things (IoT) infrastructures have been developed mostly for increasing users' entertainment and engagement experiences with cultural objects and sites (Marulli, Pareschi, & Baldacci, *The Internet of Speaking Things and Its Applications to Cultural Heritage.*, 2016), (Marulli & Vallifuoco, *The imitation game to cultural heritage: a human-like interaction driven approach for supporting art recreation*, 2016), (Amato, Di Martino, Marulli, Mazzeo, & Moscato,

2017) and for behavioral modeling and monitoring of users in cultural sites, as in museums and public exhibitions (Chianese, Marulli, Piccialli, Benedusi, & Jung, 2017), (Marulli & Vallifuoco, *Internet of things for driving human-like interactions: a case study for cultural smart environment*, 2017).

Anyway, SNs, WSNs, and IoT haven't been exploited yet at their effective potential to design and build systematic methodologies for threats prevention and vulnerabilities discovery actions, in the cultural heritage domain.

By hazard site it is intended as landslide risk zone, and cultural heritage means structure with historical value as masonry ancient construction.

It is also possible to find in the literature a large number of studies concerning the use of optical fibers in the medical field, for example in colonoscopy practices to increase patient comfort (Zhao, Soto, Tang, & Thévenaz, 2016).

Distributed strain measurements by optical fiber sensors have great advantages with respect to measurements done by traditional gauges such as resistive or mechanical ones and among others those based on Brillouin optical time-domain analysis (BOTDA) that are discussed here. (Minutolo, Esposito, Ferla, Palladino, & Zona, 2019)

As a matter of fact, life-long measurement is the new challenge in Civil Engineering, especially with respect to construction maintenance and management. It is clear that life-long monitoring requires that the sensors are positioned in situ and left in place permanently; consequently, they need to be protected from the injuries caused by time and their environment (Fajkus, et al., 2017).

Optical fibers for telecommunications, which are the sensing devices when BODTA is used, are very robust and do not suffer time degradation, but the fiber is rather fragile and requires some protection

against mechanical shocks. For the scope, it is desirable that the fiber is protected by means of coating. Different ways of coating are planned for optical fiber, they are mainly based on combinations of carbon fiber layers and glass fiber layers, depending on the mechanical characteristics required for the environment they are included. This has two main advantages: at first, protection for optical fibers and then as an instrumented reinforcement.

Barrias and Bao (Barrias, Casas, & Villalba, 2016), (Bao & Chen, 2011) describe the evolution of the SHM with a review of the major experiments and results carried out to date to demonstrate the effectiveness of the use of optical fiber sensors.

In this paper, a novel type of sensor is presented. The S.T.R.A.I.N. (that is the name chosen by authors) sensor is a transducer made by optical fiber sensors coated with fiber carbon in order to give stiffness to the transducer. The transducer is instrumented with connected technology that allows it to be always remote connected with a server, and the data acquired always available by PCs or even, smartphones, removing the need of an operator to be present in the main control center.

2 METHOD

BODTA sensors provide as output the value of the strain measured along a spatial dimension that depends on the used acquisition device. Civil engineering applications do not need a high spatial resolution, but the availability of measurements of strain and displacements, and also temperature, is very useful in order to interpret the structure's health state. In this section, a brief explanation of the method used to read the fiber's output in terms of displacements is reported. The S.T.R.A.I.N. sensor consists of an optical fiber coated with carbon fiber. The carbon fiber has the function of protecting the optical fiber, keeping it in a fixed position so that it is

possible both to obtain reliable measurements and to reinforce the monitored structures.

In the following a brief explanation of how the sensor acquires and converts data to be used for safety evaluation. To validate the present results, it is necessary the comparison between theoretical and experimental results through the choice of a constitutive relation as the explicit one of Mander et al (1988) (Mander, Priestley, & Park, 1988) introduced in the following steps.

The concrete compression stress, namely σ_c , is a function of the strain and the yield stress too.

Moreover, a measure of the yield concrete stress, named σ_{cy} , has been carried out testing a 15cmx15cmx15cm cubical specimen and resulting about -13.75 MPa.

As previously introduced, the Mander equation is adopted through a modified form as shown inside the following equations:

$$\sigma_c = \begin{cases} \sigma_c = 0 & , \varepsilon < -0.0035 \\ \sigma_c = \sigma_{cy} \frac{\varepsilon}{\varepsilon_{c0}} \frac{n}{n-1 + \left(\frac{\varepsilon}{\varepsilon_{c0}}\right)^n} & , -0.0035 < \varepsilon < -0.002 \\ \sigma_c = -(250000\sigma_{cy})\varepsilon^2 - (1000\sigma_{cy})\varepsilon & , -0.002 < \varepsilon < 0 \end{cases} \quad (1)$$

In order to perform a more accurate investigation, concrete crashes and cracks have been considered.

Moreover, the stress has been considered to vanish for tensile strain under the value of -0.0035.

Instead, the steel has been considered an elastic, perfectly plastic material with a Young's modulus $E_s = 210GPa$. In the same way of the concrete part of the structure, the steel stress yielding resulted to be:

$$\sigma_{sy} = 380MPa \quad (2)$$

The stress-strain curve linked to the steel, has the following equations (3):

$$\sigma_s = \begin{cases} \sigma_s = 0 & , \varepsilon < -0.01 \\ \sigma_s = -\sigma_{sy} & , -0.01 < \varepsilon < -0.002 \\ \sigma_s = E_s \varepsilon & , -0.002 < \varepsilon < 0.002 \\ \sigma_s = \sigma_{sy} & , 0.002 < \varepsilon < 0.01 \\ \sigma_s = 0 & , 0.01 < \varepsilon \end{cases} \quad (3)$$

Finally, the stress-strain curves for the concrete and steel, are reported in Figure 1.

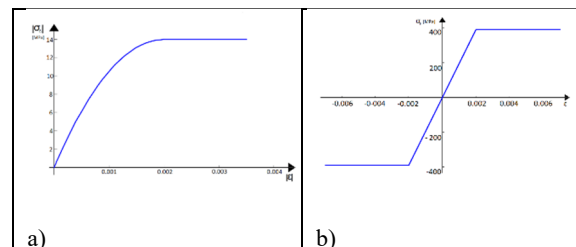


Figure 1: Stress-strain laws for a) concrete on the compressive range, b) steel.

For the previous definitions, equations (1) and (3), the moment-curvature was carried out using numerical integration of the stress-strain curves through an iterative procedure composed by the following steps:

Fix a curvature value.

Solve for the horizontal neutral axis and splitting the cross section into the parts where the stress resultants are opposite.

Integrate the stress moment along the beam thickness referring to the neutral axis.

The so obtained moment is the one corresponding to the prescribed curvature.

The results of the procedure, applied to the introduced structures, allowed to report the moment-curvature diagram drawn in Figure 2.

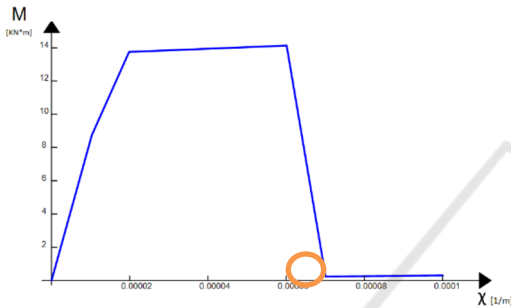


Figure 2: Bending moment versus curvature diagram.

The diagram in Figure 2 fulfills with the one proposed by Kwak and Kim (2009) (Kwak & Kim, 2010), where the three linear parts of the diagram represent pure elastic, cracked concrete and steel yield phase of the cross section respectively. The calculated cracks and crushes moments of the concrete have been carried out considering that the stress vanishes under the ultimate strain.

$$\varepsilon = 0 \text{ and } \varepsilon = \varepsilon_{c0} \tag{4}$$

As shown in the fig.7, the concrete limit corresponds to the decreasing moment

$$c = .000065 \frac{1}{m}$$

value linked to the curvature.

Moreover, a little range of residual moment can be seen in figure 2 starting from the circle to the ultimate value. This fact is linked to the steel bars that never reach their failure point for the curvature here considered.

Starting from known values of stress and strain, it has been possible to derive a curvature-moment diagram using a numerical procedure that consists of the integration of the curvature-moment relationship imposing the normal effort equal to zero and carrying out the height of the neutral axis to be input.

A curvature range is defined as follows:

$$\chi_{max} = \frac{10^{-6}}{h/2}$$

$$\chi_{min} = \frac{10^{-2}}{h/2} \tag{5}$$

Within this range a certain curvature value of the cross section has been imposed:

$$\chi_{min} \leq \chi \leq \chi_{max} \tag{6}$$

which will be given by the equation:

$$\chi = \chi_{max} \cdot t + (1 - t) \cdot \chi_{min} \tag{7}$$

With

$$t = \frac{i}{i_{max}} \tag{8}$$

For each bending moment value inside the interval (6) the deformation trend is evaluated as follow:

$$\varepsilon(y) = \chi \cdot (y - y_n) \tag{9}$$

Starting from it, the stresses are obtained fulfilling the equations (1) and (2) parameterized with respect to the neutral axis depth. From the resultant stress and moment values, the depth of the neutral axis has been determined by searching the solution in a numerical way of the equilibrium equation along the beam axis:

$$N(y_n) = \int \sigma(\varepsilon) d\varepsilon = 0 \tag{10}$$

By the end, the corresponding normal stress is obtained for each value of the curvature. Moreover, for the hypotheses of the Euler-Bernoulli beam theory, the normal stress must have a zero value for each depth of the neutral axis, except for fluctuations due to the numerical algorithm.

Through the numerical quadrature of the stresses, the bending moment has been obtained:

$$M(\chi) = \int \sigma(\varepsilon) \cdot (y - y_n) d\varepsilon \tag{11}$$

In Figure 2, has been reported the numerical values of the bending moment as a function of the curvature of the cross section.

The maximum moment calculated is:

$$M_m = 14.20 \text{ kNm} \tag{12}$$

The theoretical value of the limit moment allows us to calculate the limit load, as

$$M_y = F_y d \Leftrightarrow F_y = \frac{M_y}{d} \tag{13}$$

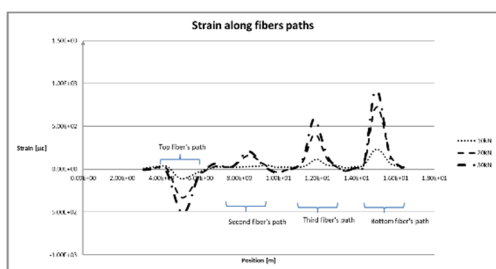


Figure 3: Strain Along fiber paths.

By using the initial quantity:

$$d = 0.73m - 0.26m = 0.47m \tag{14}$$

$$F_y^M = \frac{14.20kNm}{0.47m} = 30.21kN \tag{15}$$

From equation (13) the yield force can be assumed about 30 kN.

In the following Table 5, the fiber optic strains at sections located at the mid-span of the beam, i.e. at a distance z from the left-wise support given by $z = 0.91$ m (see Figure 4), are reported; In particular, in the table, the beam curvature and bending moment, calculated analytically from recorded data, are reported as well. By assuming that the Bernoulli hypothesis holds, the curvature is calculated by

$$\chi = \frac{\epsilon_l - \epsilon_u}{h - c} \tag{16}$$

here $h - c$ is the distance between the top and fourth fiber bar path along the cross-section height, which also corresponds to the distance between the two rebar sets. The reported value $c = 20mm$ is the distance of the bars from the upper and the lower side of the section, h is the distance between the lower bar path and the upper side of the beam, ϵ_u and ϵ_l are the strains of the upper and lower bar path respectively. As previously described, in the present experiment, a single fiber string with a length of about 18 meters was introduced inside the beam. The fiber has been fixed to the reinforcements in a phase preceding the casting one, and it runs along the beam four times in four different positions according to 4 paths (top path, second path, third path, bottom path) as shown in figure 3. This Figure represents a diagram showing the value of the deformations measured by the fiber along its entire length. On the abscissa the whole length of the fiber is reported; in order to know the value of the deformation measured in the specific position of the beam, it is necessary to read it on the single path which describes the value of the deformation according to the position where the fiber is installed.

3 BIG DATA AND EARLY WARNINGS

This section explains how the proposed system could be useful in landslide risk and SHM in lifetime analysis, in self-learning of parameters of early warning.

A lifetime monitored structure or soil generates a great number of information in terms of strain.

As it has been shown in this contribution, this information can be converted in terms of curvature and displacements. This last information is needed in order to evaluate the safety of soils and structure in a conventional way.

In the very first instance, an evaluation of this type is useful on structures or soils that show evident signs of subsidence; therefore, it is suitable for immediate intervention. This is the case explained in the previous section.

However, things change when one decides to monitor a structure or a soil that is apparently or actually in a healthy state for its entire lifetime.

In this case, the sensor presented in this paper is able to furnish information about strain, displacements, and curvature continuously in time and also in remote control.

This means that it is possible to check the status of the displacement at every moment. The status is always available because the sensor can be connected to the internet, in order to make data disposable on a server, a notebook or a smartphone.

This allows the user to know the static state of a structure at every moment. Moreover, the user, is indispensable only in the warning phase, because the system is able to detect anomalies autonomously. For instance, the system can avoid false alarms due to peaks in strain, displacements, and curvatures.

Such a monitoring system represents a network of sensors that are both signal and medium.

With the knowledge of the theoretical models described in the previous section, it is possible to filter the information by creating an early warning smart system that, as the data collected approaches a critical situation, allows to activate alerts that prevent environmental disasters, or less drastically, which leads to extraordinary maintenance that has less impact on large structures, soils, and culturally valuable assets.

In addition, a type of model is acquired that is independent of experimental evidence by providing an approach based on a time history analysis. In fact, the system automatically recognizes the risk values to which the structure or instrumented soils are approaching. In this way, no type of numerical or

analytical analysis is necessary, but the intelligent monitoring system foresees the risk.

4 CONCLUSIONS

This system allows reaching different aims simultaneously.

The big data collection leads to collect a load history of the structure and soil movements. By doing so, one can forecast, not only regular load cycles but also load peaks due to extraordinary loads that do not lead the structure to failure, i.e. high loaded trucks (for streets) or trains (for railways), cranes for maintenance work, etc. In this condition, false alarms can be bypassed easily, by only warning the user when needed.

But even if there is no warning, this system allows the user to monitor the optical fiber continuous data by real time information provided by the system.

Thanks to a smartphone application, all this information can be reached not only by the main control center in a fixed time and place but pretty much whenever and everywhere with the handy and most used device nowadays.

ACKNOWLEDGMENTS

The authors deeply acknowledge the contribution of the financial grant VALERE: “VANviteLli pEr la RicErca”.

REFERENCES

- Amato, F., Di Martino, B., Marulli, F., Mazzeo, A., & Moscato, F. (2017). A Target Driven Approach Supporting Data Diversified Generation in IoT Applications. Springer, (p. 825--833).
- Bao, X., & Chen, L. (2011, 6 19). Recent progress in optical fiber sensors based on Brillouin scattering at university of Ottawa. *Photonic Sensors*, 1(2), 102-117.
- Barrias, A., Casas, J., & Villalba, S. (2016, 5 23). A Review of Distributed Optical Fiber Sensors for Civil Engineering Applications. *Sensors*, 16(5), 748.
- Chianese, A., Marulli, F., Piccialli, F., Benedusi, P., & Jung, J. (2017). An associative engines based approach supporting collaborative analytics in the internet of cultural things. *Future generation computer systems*, 66, 187--198.
- Fajkus, M., Nedoma, J., Mec, P., Hrubesova, E., Martinek, R., & Vasinek, V. (2017, 9 1). Analysis of the highway tunnels monitoring using an optical fiber implemented into primary lining. *Journal of Electrical Engineering*, 68(5), 364-370.
- Housner, G., Bergman, L., Caughey, T., Chassiakos, A., Claus, R., Masri, S., . . . Yao, J. (1997, 9). Structural Control: Past, Present, and Future. *Journal of Engineering Mechanics*, 123(9), 897-971.
- Kwak, H.-G., & Kim, S.-P. (2010, 1). Simplified monotonic moment–curvature relation considering fixed-end rotation and axial force effect. *Engineering Structures*, 32(1), 69-79.
- Mander, J., Priestley, M., & Park, R. (1988, 9). Theoretical Stress-Strain Model for Confined Concrete. *Journal of Structural Engineering*, 114(8), 1804-1826.
- Marulli, F., & Vallifuoco, L. (2016). The imitation game to cultural heritage: a human-like interaction driven approach for supporting art recreation. *Interactivity, Game Creation, Design, Learning, and Innovation*, p. 145--153.
- Marulli, F., & Vallifuoco, L. (2017). Internet of things for driving human-like interactions: a case study for cultural smart environment., (p. 1--9).
- Marulli, F., Pareschi, R., & Baldacci, D. (2016). The Internet of Speaking Things and Its Applications to Cultural Heritage., (p. 107--117).
- Minutolo, V., Esposito, L., Ferla, P., Palladino, S., & Zona, R. (2019). NON LINEAR STRAIN MEASURES ON CONCRETE STRUCTURES BY MEANS OF EMBEDDED OPTICAL FIBER SENSORS. *International Journal of Civil Engineering and Technology (IJCIET)*, 10, 10-12.
- Zhao, Z., Soto, M., Tang, M., & Thévenaz, L. (2016, 10 31). Distributed shape sensing using Brillouin scattering in multi-core fibers. *Optics Express*, 24(22), 25211.